Available online at www.sciencedirect.com

SciVerse ScienceDirect

Ceramics International 39 (2013) 5103–5111

CERAMICS INTERNATIONAL

www.elsevier.com/locate/ceramint

Evaluation of stress distribution and failure mechanism in lanthanum–titanium–aluminum oxides thermal barrier coatings

Musharaf Abbas[a], Lei Guo[a], Hongbo Guo[a,b,*]

[a]School of Materials Science and Engineering, Beihang University, No. 37, Beijing 100191, China
[b]Beijing Key Laboratory for Advanced Functional Material and Thin Film Technology, Beihang University, No. 37, Xueyuan Road, Beijing 100191, China

Received 1 October 2012; received in revised form 30 November 2012; accepted 3 December 2012
Available online 20 December 2012

Abstract

$LaTi_2Al_9O_{19}$ (LTA) is one of the most promising materials for new thermal barrier coatings (TBCs) to fulfill the demand of advanced gas turbines owing to its high temperature stability and low thermal conductivity. In the present study, a finite element (FE) based numerical study has been carried out to investigate the stress distribution in LTA single layered coating system in comparison with traditional yttria stabilized zirconia (YSZ) TBC. Stresses in YSZ/LTA double ceramic layer TBC system are also determined and presented for comparative analysis. The thermal cycling effect is simulated by sequent increment in TGO thickness in a series of FE simulations. In-plane stresses (σ_{xx}), out-of-plane stresses (σ_{yy}) and shear stresses (σ_{xy}) are determined for all systems, and peak stress values are presented for quantitative comparison. Elastic strain energy stored in TGO of all systems is calculated from FE results for TBC structural integrity assessment. It has been found that maximum in-plane and shear stresses are lower in the double ceramic layer coating system than in the single layer ceramic coating system. However, peak axial tensile and compressive stresses in the double ceramic layer coating are very close or higher than those in the single layer topcoat. Calculation of elastic store energy shows that double ceramic layer TBC system may exhibit better stability as compared to single layer systems. Results are presented to explain the failure mechanism in LTA coatings.

Keywords: Thermal barrier coatings (TBC); $LaTi_2Al_9O_{19}$ (LTA); Residual stress; Finite element method

1. Introduction

Thermal barrier coatings (TBCs) have successfully been used in thermally highly loaded metallic components, as for instance in gas-turbine engine blades and vanes to protect them from hot burner gases, leading to further increase in operating temperature and thus to increase the efficiency of turbine engines [1–5]. The requirements to improve jet engine efficiencies have proved to be a big driving force to improve the thermal barrier coating technology by novel compositions and improved production techniques for subsequent improvement in microstructure and thus to enhance thermo-mechanical performance of TBCs. Yttria stabilized zirconia (YSZ) is the present industrial standard topcoat material in TBC system, which can operate long term at temperatures below 1200 °C [1,4,6]. The limited capability of YSZ above 1200 °C necessitates its substitution with some novel compositions capable of handling higher temperatures with better stability in advanced gas turbines. A number of ceramic materials, mostly oxides, have been proposed as novel thermal barrier coatings during the last few years. These novel compositions cover especially doped zirconia [7,8], pyrochlores [9–11], aluminates [12–14] and perovskites [15,16].

Recently, $LaTi_2Al_9O_{19}$ (LTA) has been investigated as one of TBC candidate materials because of its better thermal properties and excellent high-temperature stability for application up to 1500 °C [17–20]. LTA has a face-centered monoclinic crystallographic structure with a unit cell that is

*Corresponding author at: School of Materials Science and Engineering, Beihang University, No. 37, Beijing 100191, China.
Tel./fax: +86 10 8231 7117.
E-mail address: guo.hongbo@buaa.edu.cn (H. Guo).

0272-8842/$ - see front matter © 2012 Elsevier Ltd and Techna Group S.r.l. All rights reserved.
http://dx.doi.org/10.1016/j.ceramint.2012.12.006

four times as large as that of the magnetoplumbite phase and interleaved with pseudobrookite-like layers. The special crystallographic sites allow achieving the capability of a lower thermal conductivity in LTA [19].

Previous research on LTA as TBC material mainly covers its thermo-physical and mechanical properties and its thermo-chemical stability at higher temperatures [17–20]. However, there is very limited to virtually no data

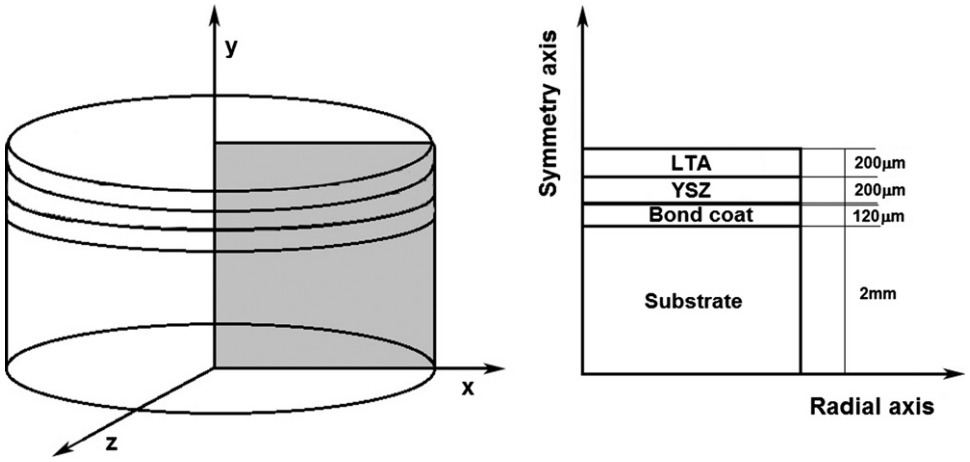

Fig. 1. Schematic illustration of the geometric model.

Table 1
Material performance parameters of substrate, bond coat, TGO, YSZ and LTA ceramic topcoats [2,19,21].

Material	Temperature (°C)	Young's modulus (GPa)	Poisson's ratio	Thermal expansion coefficient ($\times 10^{-6}$ °C^{-1})	Thermal conductivity (W m^{-1} °C^{-1})
Ni based alloy (substrate)	20	220	0.31	14.8	88
	200	210	0.32	15.2	73.3
	400	190	0.33	15.6	59.5
	600	170	0.33	16.2	62
	800	155	0.34	16.9	65
	1000	130	0.35	17.5	68.1
	1100	120	0.35	18	69
NiCrAlY (bond coat)	20	200	0.3	13.6	5.8
	200	190	0.3	14.2	7.5
	400	175	0.31	14.6	9.5
	600	160	0.31	15.2	12
	800	145	0.32	16.1	14.5
	1000	120	0.33	17.2	16.2
	1100	110	0.33	17.6	17
Al_2O_3 (thermally grown oxide)	20	400	0.23	8	10
	200	390	0.23	8.2	7.794
	400	380	0.24	8.4	6.029
	600	370	0.24	8.7	5.074
	800	355	0.25	9	4.412
	1000	325	0.25	9.3	4.412
	1100	320	0.25	9.6	4
YSZ (top coat)	20	48	0.1	9	1.956
	200	47	0.1	9.2	1.834
	400	44	0.1	9.6	1.736
	600	40	0.11	10.1	1.627
	800	34	0.11	10.8	1.634
	1000	26	0.12	11.7	1.681
	1100	22	0.12	12.2	1.7
LTA (top coat)	20	113	0.22	7.7	1.307
	200	108	0.22	7.74	1.331
	400	103	0.23	8.67	1.280
	600	100	0.23	9.31	1.266
	800	97	0.24	9.59	1.271
	1000	92	0.24	10.28	1.043
	1100	86	0.24	10.41	1.098

available on stress distribution in LTA TBCs especially with increasing TGO thickness as a function of thermal exposure time, which is necessary to investigate the failure mechanism in LTA coatings. Since TBC is a multilayer system comprised of different classes of materials, its structural integrity assessment is a major concern owing to the different thermo-mechanical response of each material of the system. The intent of this article is to investigate the mechanical response of the TBCs under the thermal load effect to evaluate the thermo-mechanical stability of the system. A numerical based study has been carried out for comparative analysis of the stress distribution in the single layer YSZ, LTA and double layer YSZ/LTA TBC systems over a range of TGO thickness (1–10 μm). Stress states in all TBC systems are evaluated by calculating elastic strain energy in each system for structural integrity assessment. Results are compared with previous studies on thermal life and failure of LTA coatings to explain the failure mechanism with regard to stress state in these coating systems.

2. Finite element model

In the present model, circular disc specimen is considered, allowing the problem to be reduced to a two-dimensional axisymmetric case in the radial and through thickness directions as schematically shown in Fig. 1. TBC system is comprised of four layers in single-ceramic-layer system and in the double-ceramic-layer system an additional layer is present at the top. Thicknesses of substrate, bondcoat, TGO and single layer topcoats are 2 mm, 120 μm, 1–10 μm (varying parameter) and 200 μm respectively. In double-ceramic-layer coating, both layers are 200 μm thick. A coupled thermo-mechanical finite element solution has been employed using 2-D coupled field element PLANE223. Element PLANE223 has eight nodes with up to maximum four degrees of freedom per node. Due to the solid model entities, mapped grid is selected for mesh construction as it generates regular and thus computationally well-behaving, meshes. Geometry consists of approximately 25,000–30,000 elements depending on single and double layer ceramic coats. Due to the relatively smaller area of TGO, the TGO and the surroundings regions are finely meshed to enhance the sensitivity of the model to the rigorous changes in stress distribution in this region. The model has total five materials: Ni-based superalloy substrate, NiCoCrAlY bond-coating, Al_2O_3 thermally grown oxide (TGO), YSZ and LTA ceramic topcoats. Thermal and mechanical properties at varying temperatures of the materials used in the analysis are obtained from literature [19,21] and are given in Table 1. Due to axisymmetric configuration of the model, symmetric boundary conditions are used. The TBC model is subjected to a uniform thermal load through a drop in the temperature from an assumed stress free state at 1050 °C to room temperature of 25 °C. All layers are considered homogeneous and isotropic. Heat convection is imposed on the top of the sample while the bottom of the specimen is assumed to be thermally insulated. Mechanisms such as phase transformation and creep that can affect thermal stresses are assumed to be inactive during the simulation. Peak radial tensile and compressive stresses, maximum axial stresses and shear stresses within TBCs for all TBC systems have been determined.

3. Results and discussion

3.1. In-plane stresses

Fig. 2 shows variation in peak tensile in-plane stress as a function of TGO thickness for all coating systems. These in-plane stresses exist at the bond coat/TGO interface near the edge of the specimen in all cases. Figure shows that peak tensile radial stress increases by the increase in TGO thickness, and it is lower in double-layer-ceramic TBC system as compared to single YSZ and LTA coating systems. Stresses in single YSZ coating are lower than in the LTA coating system. A prominent stress difference of

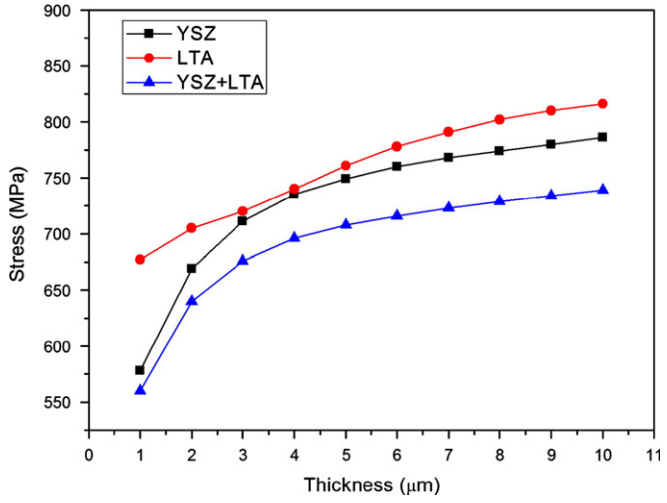

Fig. 2. Radial tensile stress in YSZ, LTA and YSZ/LTA coating systems as a function of TGO thickness.

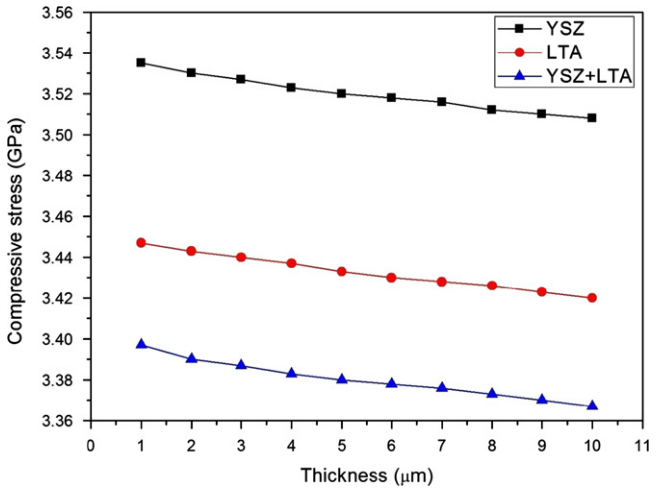

Fig. 3. Radial compressive stress in YSZ, LTA and YSZ/LTA coating systems as a function of TGO thickness.

about 120 MPa exists between single layer LTA coating and double ceramic layer coating at minimum TGO thickness. Fig. 3 shows residual compression stresses for considered TGO thickness range for all TBC systems. These stresses are developed due to the difference in thermal expansion between TGO layer and bond coat. Fig. 3 shows that compressive stresses for all TBCs drop proportionally with the increase in TGO thickness. In-plane compressive stresses in double layer ceramic coating system are lower than in single layer systems. Between single layer LTA and YSZ coatings, the stresses in the LTA coating are lower than in the YSZ coating system. For further details, in-plane stress distribution for two TGO thicknesses, 1 μm and 7 μm, for all TBC systems is shown in Fig. 4. It shows that the stress distribution in all cases is almost same with the same peak stress locations. However, the difference exists in maximum stress values, which vary with the type of topcoat and with the increase

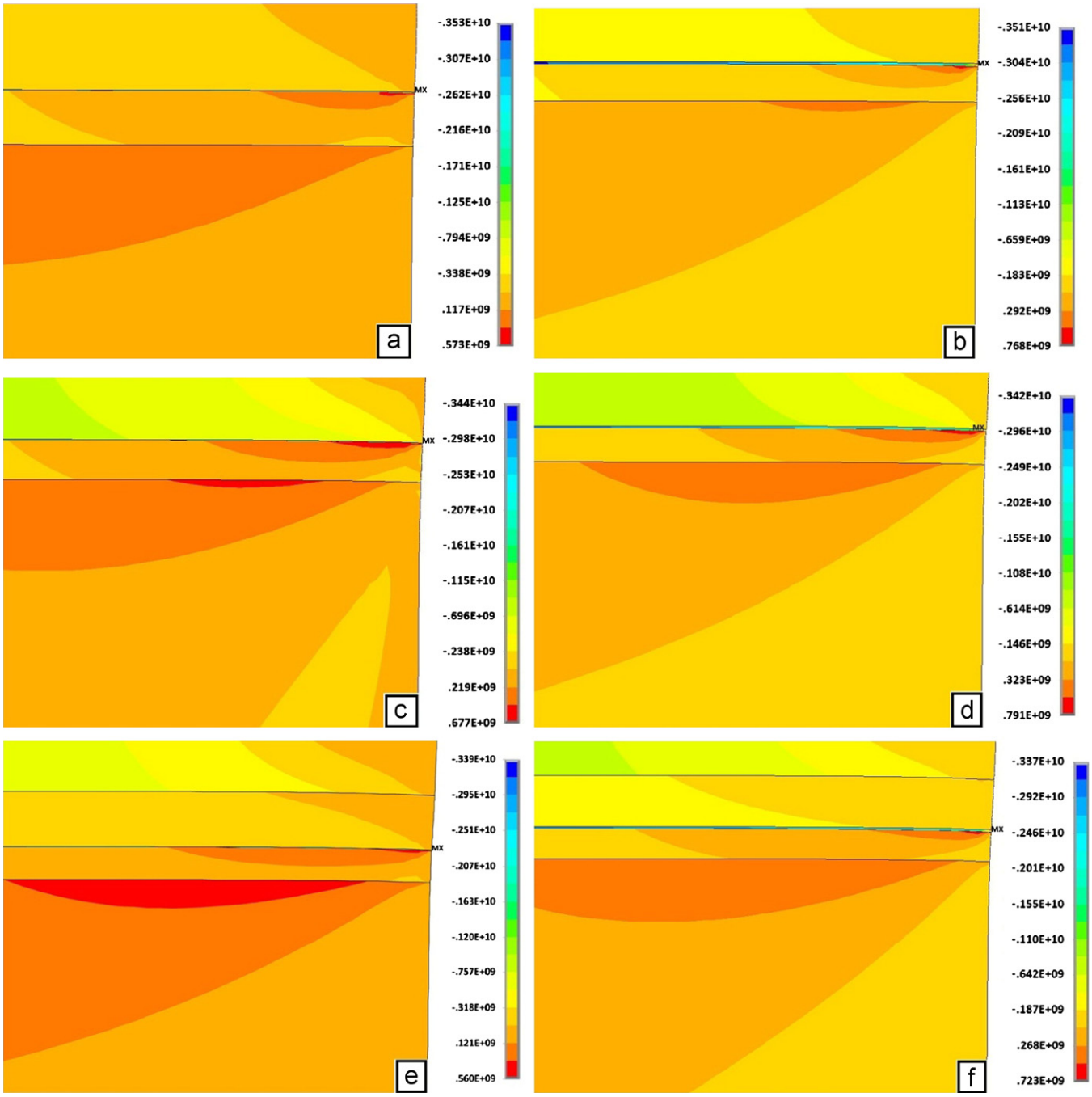

Fig. 4. Contour plot of in-plane stress (σ_{xx}) distribution in YSZ coatings (a, b), LTA coating (c, d) and YSZ/LTA coating (e, f) at 1 μm (left) and 7 μm (right) TGO thicknesses.

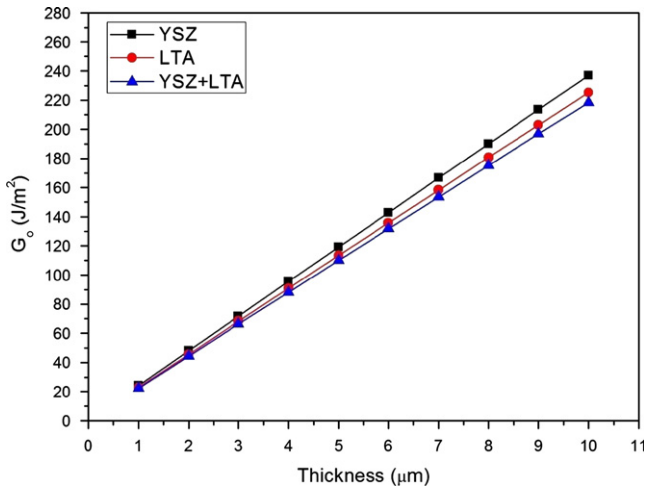

Fig. 5. Elastic strain energy within TGO for YSZ, LTA and YSZ/LTA coating systems.

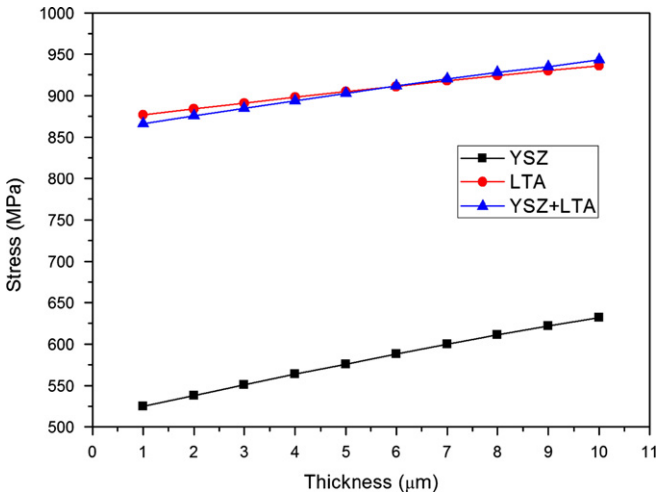

Fig. 7. Axial compressive stresses in YSZ, LTA and YSZ/LTA coating systems as a function of TGO thickness.

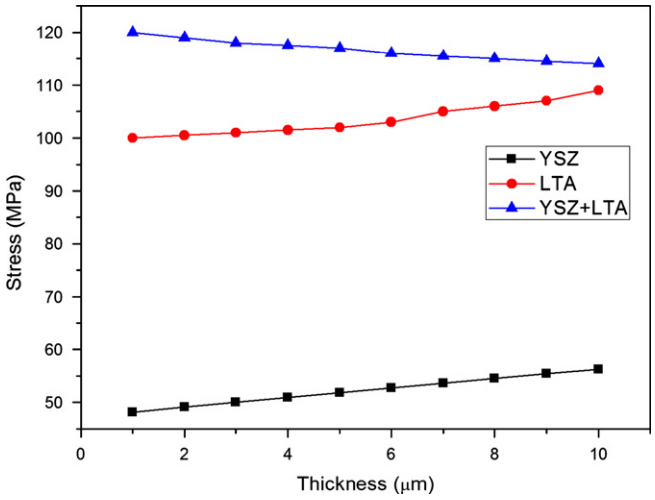

Fig. 6. Axial tensile stresses in YSZ, LTA and YSZ/LTA coating systems as a function of TGO thickness.

in the TGO thickness. The maximum tensile radial stress is significant because it exists at the bondcoat/TGO interface near the edge and in bondcoat region as shown in Fig. 4. Since TGO is under compression, this stress state may lead to mode II cracking and thus plays an important role in edge delamination and in eventual spallation.

The durability of the TBC is controlled by the energy density in the TGO and is analyzed by calculating the total elastic strain energy per unit area [22]. The elastic energy per unit area in the unbuckled film (G_o) increases proportionally with oxide thickness h_{ox} and in-plane compressive stress σ_{ox} and is given as follows [23]:

$$G_o = ch_{ox}\sigma_{ox}^2 \quad (1)$$

where $c=(1-v_{ox})/E_{ox}$, and v_{ox} and E_{ox} are Poisson's ratio and elastic modulus of TGO respectively. For Al_2O_3 oxide film, $c=1.925\times10^{-12}$. TGO failure is possible if G_o exceeds Γ_o, where Γ_o is the fracture toughness of the interface [24]. The elastic strain energy G_o for all coating systems has been computed from the numerically calculated stress value in TGO from finite element (FE) analysis for TBC durability assessment. The results for elastic strain energy G_o are presented in Fig. 5. Fig. 5 shows that the elastic strain energy stored in TGO for YSZ/LTA coating system is slightly low as compared to single YSZ and LTA coatings, especially at higher TGO thickness, while maximum energy stored is observed in the YSZ system that is about 20 J/m^2 higher than in YSZ/LTA double ceramic layer coating. Stress state and low elastic strain energy present in double layer ceramic coating system also comply with past studies which show that thermal cycle life of YSZ/LTA double ceramic layer coating systems is higher than single layer YSZ or LTA coating systems [19].

3.2. Out-of-plane stresses

Variation in normal stresses as a function of TGO thickness in YSZ, LTA and YSZ/LTA coating systems is shown in Fig. 6. Figure shows that different from in-plane stresses, the largest normal stresses exist in double layer ceramic coating system, which decrease with the TGO thickness. However these peak stresses are not considerably high and do not exist at any interface, thus may be less detrimental to TBC as compared to radial stresses existing in critical regions, in TGO and at interfaces. Moreover, stresses in YSZ coating system are lower than in YSZ/LTA coating with a maximum difference of about 70 MPa at minimum TGO thickness at which the radial stresses are lowest in double ceramic layer coatings. Variation in axial compressive stresses in YSZ, LTA and double ceramic layer YSZ/LTA coatings is shown in Fig. 7, which shows that axial compressive stresses in LTA and YSZ/LTA coating systems are nearly equal with a slight difference at minimum and maximum TGO thicknesses considered in this study.

However, the stresses in YSZ single layer coating system are lower than in the other two coatings with a difference of approximately 350 MPa. Stress state in normal direction is further elaborated in Fig. 8 with the contour plot of axial stress for 1 μm and 7 μm TGO thickness cases. Fig. 8 shows that maximum axial tensile stress in the YSZ coating system exists in substrate, while in LTA and YSZ/LTA systems it lies in LTA layer near the edge of the sample close to the interface. These stresses in LTA coatings normal to the interface may play some important role in initiation of cracks and then its propagation in the course of thermal exposure and ultimately may result in failure of the TBC system. Similar observations have been reported by Xie et al. [25] in which chipping spallation has been reported in YSZ/LTA system owing to the cracks developed in the LTA layer. The axial compressive stresses, however, exist in substrate at the edge of the specimen near the substrate/bondcoat interface in all cases. It is reported in literature that the oxides at the substrate/bondcoat interface are believed to be of spinel type [26,27] giving the interface poor mechanical properties and thus any stress state in this vicinity may also be an important consideration.

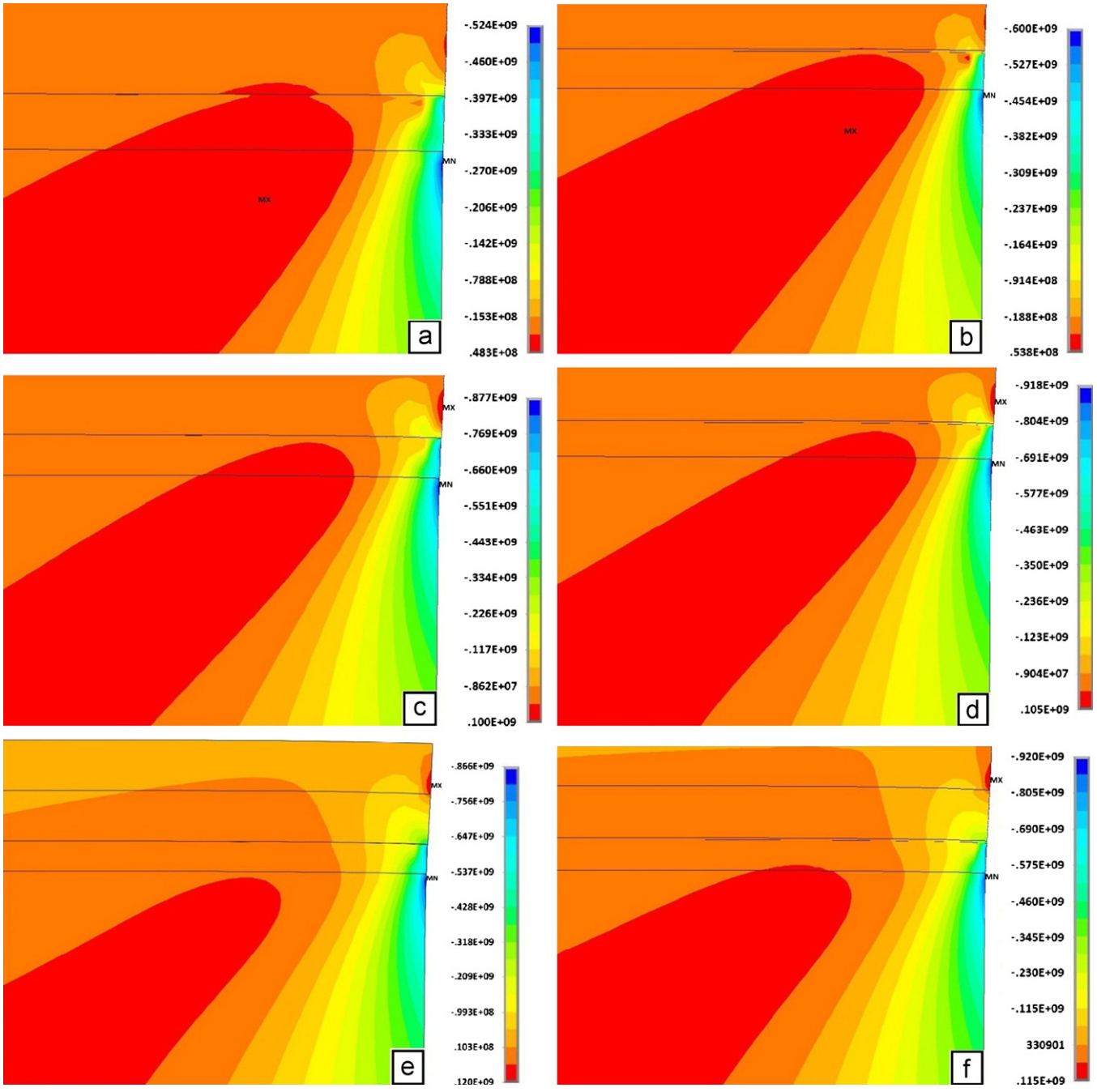

Fig. 8. Contour plot of normal stress (σ_{yy}) distribution in YSZ coatings (a, b), LTA coating (c, d) and YSZ/LTA coating (e, f) at 1 μm (left) and 7 μm (right) TGO thicknesses.

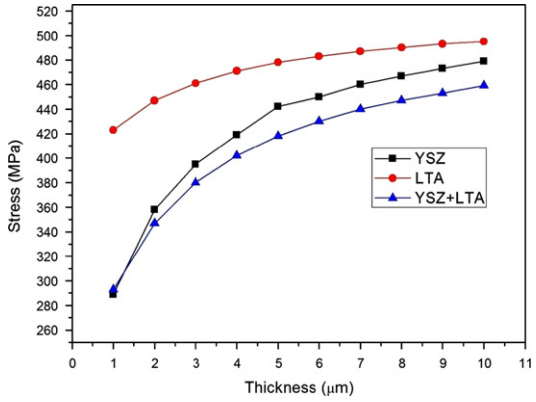

Fig. 9. Shear stresses in YSZ, LTA and YSZ/LTA coating systems as a function of TGO thickness.

3.3. Shear stresses

Variation in shear stress in all coating systems with varying TGO thickness is shown in Fig. 9. Figure shows that shear stress increases with the increase in TGO thickness in all coating systems. However, these stresses in LTA coating system are higher than in YSZ and YSZ/LTA coating systems specifically at lower TGO thicknesses. The minimum shear stresses exist in 1 μm thick TGO case in YSZ and double ceramic layer YSZ/LTA coating systems with a difference of about 130 MPa from single layer LTA coating. From 2 μm TGO growth, the shear stress in the YSZ coating system becomes higher than in double ceramic layer coating system, and the difference keeps on increasing up to 5 μm where the

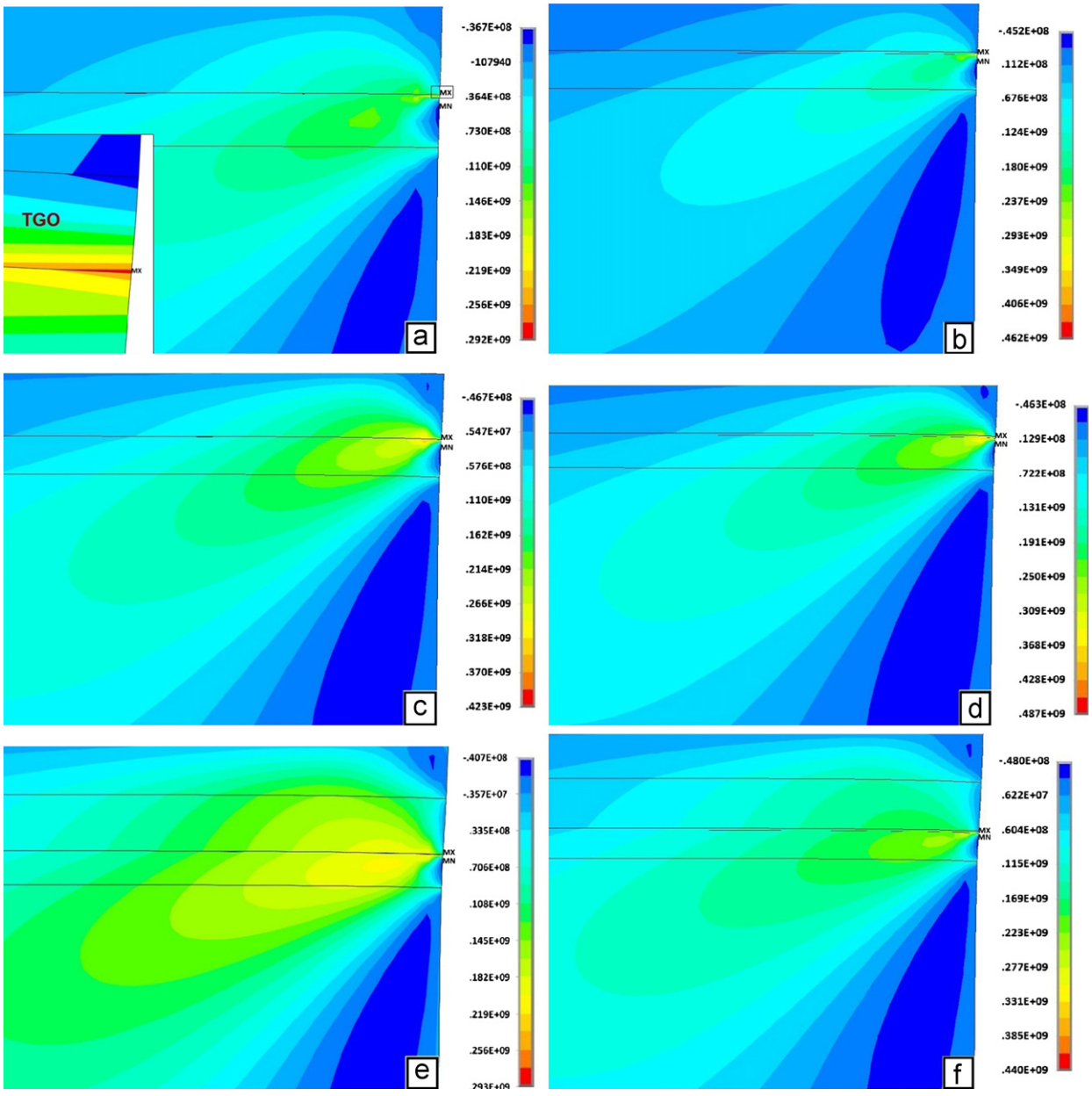

Fig. 10. Contour plot of shear stress (σ_{xy}) distribution in YSZ coatings (a, b), LTA coating (c, d) and YSZ/LTA coating (e, f) at 1 μm (left) and 7 μm (right) TGO thicknesses.

maximum difference is approximately 20 MPa and then it is constant with subsequent TGO growth. Shear stress distribution in YSZ, LTA and YSZ/LTA coating systems for 1 μm and 7 μm TGO thickness cases is presented in Fig. 10. Figure shows that location of peak stresses in all cases is the same that is the TGO/bondcoat interface. Difference lies only in peak stress value, which has been explained in Fig. 9. This stress state is important as initiation of an interface separation is contingent upon the existence of a shear stress at the interface [28]. Moreover, TGO bonded to its substrate sustains large in-plane residual stresses (in this study 3.3–3.5 GPa range) that are transferred to the TGO via shear stresses on the interface near their edges, and these edge zones play a significant role in TGO delamination [29]. Fig. 9 suggests that double layer ceramic coat system is more resistant to shear stress driven failure, especially with TGO growth during the course of thermal exposure.

FEM results with subsequent analysis suggest that double ceramic layer (YSZ/LTA) TBC system is a promising candidate for TBC applications, owing to the stress state developed in it in comparison with other systems. This finding is also substantiated from experimental investigations by Xie et al. [19], who found YSZ/LTA to be a long thermal life material as compared to single layer YSZ or LTA coating systems. An additional benefit of using LTA coating systems over traditional YSZ coating is its capability to be used at higher temperatures above 1250 °C. Future work is directed toward failure mechanics of LTA TBCs, paying special attention to interface stresses in conjunction with interface fracture toughness for more elaborative failure mechanism study.

4. Conclusions

In summary, the present study investigates the stress response of $LaTi_2Al_9O_{19}$ (LTA) TBCs under the thermal load effect. A numerical based study has been carried out for comparative analysis of the stress distribution in the YSZ, LTA and YSZ/LTA TBC systems over a range of TGO thicknesses (1–10 μm). Thermo-mechanical integrity of all TBC systems is assessed by calculating elastic strain energy in each system. Maximum in-plane tensile and compressive stresses that are important in controlling buckling instability and spallation of TBC are lowest in YSZ/LTA double ceramic layer coating system. Shear stresses are also low in YSZ/LTA coating system as compared to single layer YSZ or LTA systems. The out-of-plane stresses in all systems are not very high; however, these stresses in single layer LTA system and in double layer YSZ/LTA system exist in LTA layer near the edge and may cause cracking and ultimately failure of LTA coating systems. Axial stresses in YSZ/LTA coating system are either close to or higher than both single layer ceramic coating systems with a prominent difference in stress when compared with single YSZ coating. Elastic strain energy (G_o) associated with stress state within TGO is also low in double layer ceramic coating system, which suggests that YSZ/LTA double ceramic layer coating system may endure more thermal cycles as compared to single YSZ or LTA systems and thus its thermal life should be higher than single layer systems considered in the study.

References

[1] R.A. Miller, Current status of thermal barrier coatings—an overview, Surface and Coatings Technology 30 (1987) 1.

[2] M. Abbas, H.B. Guo, M.R. Shahid, Comparative study on effect of oxide thickness on stress distribution of traditional and nanostructured zirconia coating systems, Ceramics International 39 (2013) 475–481.

[3] J. Wu, Hongbo. Guo, M. Abbas, S. Gong, Evaluation of plasma sprayed YSZ thermal barrier coatings with the CMAS deposits infiltration using impedance spectroscopy, Progress in Natural Science: Materials International 22 (2012) 40.

[4] N.P. Padture, M. Gell, E.H. Jordan, Thermal barrier coatings for gas-turbine engine applications, Science 296 (2002) 280.

[5] R. Vaβen, M.O. Jarligo, T. Steinke, D.E. Mack, D. Stöver, Overview on advanced thermal barrier coatings, Surface and Coatings Technology 205 (2010) 938.

[6] F. Cernuschi, P. Bianchi, M. Leoni, P. Scardi, Thermal diffusivity/microstructure relationship in Y-PSZ thermal barrier coatings, Journal of Thermal Spray Technology 8 (1999) 102.

[7] M.N. Rahaman, J.R. Gross, R.E. Dutton, H. Wang, Phase stability, sintering and thermal conductivity of plasma-sprayed ZrO_2–Gd_2O_3 compositions for potential thermal barrier coating applications, Acta Materialia 54 (2006) 1615.

[8] M. Matsumoto, N. Yamaguchi, H. Matsubara, Low thermal conductivity and high temperature stability of ZrO_2–Y_2O_3–La_2O_3 coatings produced by electron beam PVD, Scripta Materialia 50 (2004) 867.

[9] H. Lehmann, D. Pitzer, G. Pracht, R. Vassen, D. Stöver, Journal of the American Ceramic Society 86 (2003) 1338.

[10] J.H. Yu, H.Y. Zhao, S.Y. Tao, X.M. Zhou, C.X. Ding, Thermal conductivity and thermal expansion coefficients of the lanthanum rare-earth-element zirconate system, Journal of the European Ceramic Society 30 (2010) 799.

[11] R. Vaβen, X. Cao, F. Tietz, D. Basu, D. Stöver, Zirconates as new materials for thermal barrier coatings, Journal of the American Ceramic Society 83 (2000) 2023.

[12] X.L. Chen, Y.F. Zhang, X.H. Zhong, J.F. Zhang, Y.L. Cheng, Y. Zhao, et al., Thermal cycling behaviors of the plasma sprayed thermal barrier coatings of hexaluminates with magnetoplumbite structure, Journal of the European Ceramic Society 30 (2010) 1649.

[13] N.P. Bansal, D.M. Zhu, Thermal properties of oxides with magnetoplumbite structure for advanced thermal barrier coatings, Surface and Coatings Technology 202 (2008) 2698.

[14] X.Q. Cao, Y.F. Zhang, J.F. Zhang, X.H. Zhong, Y. Wang, H.M. Ma, et al., Failure of the plasma-sprayed coating of lanthanum hexaluminate, Journal of the European Ceramic Society 28 (2008) 1979.

[15] H.B. Guo, H.J. Zhang, G.H. Ma, S.K. Gong, Thermo-physical and thermal cycling properties of plasma-sprayed $BaLa_2Ti_3O_{10}$ coating as potential thermal barrier materials, Surface and Coatings Technology 204 (2009) 691.

[16] W. Ma, D. Mack, J. Malzbender, R. Vaβen, D. Stöver, Yb_2O_3 and Gd_2O_3 doped strontium zirconate for thermal barrier coatings, Journal of the European Ceramic Society 28 (2008) 3071.

[17] X.Y. Xie, H.B. Guo, S.K. Gong, H.B. Xu, Hot corrosion behavior of double-ceramic-layer $LaTi_2Al_9O_{19}$/YSZ thermal barrier coatings, Chinese Journal of Aeronautics 25 (2012) 137.

[18] H.B. Guo, X.Y. Xie, H.B. Xu, et al., The manufacturing of thermal barrier coating with columnar grain structure, China Patent 200710118236.5, 2007-07-03.
[19] X.Y. Xie, H.B. Guo, S.K. Gong, H.B. Xu, Lanthanum–titanium–aluminum oxide: a novel thermal barrier coating material for applications at 1300 °C, Journal of the European Ceramic Society 31 (2011) 1677.
[20] X.Y. Xie, H.B. Guo, S.K. Gong, Mechanical properties of $LaTi_2Al_9O_{19}$ and thermal cycling behaviors of plasma sprayed $LaTi_2Al_9O_{19}$/YSZ thermal barrier coatings, Journal of Thermal Spray Technology 19 (2010) 1179.
[21] A. Liu, Y. Wei, Finite element analysis of anti-spallation thermal barrier coatings, Surface and Coatings Technology 165 (2003) 154.
[22] S. Bose, High Temperature Coatings, First ed., Butterworth–Heinemann, Elsevier, USA, 2007.
[23] J.W. Hutchinson, M.D. Thouless, E.G. Liniger, Growth and configuration stability of circular, buckling-driven film delaminations, Acta Metallurgica et Materialia 40 (1992) 295.
[24] P.K. Wright, A.G. Evans, Mechanisms Governing the Performance of Thermal Barrier Coatings, Princeton Materials Institute Report PMI-99-11, Princeton University, New Jersey, 1999.
[25] X.Y. Xie, H.B. Guo, S.K. Gong, H.B. Xu, Thermal cycling behavior and failure mechanism of $LaTi_2Al_9O_{19}$/YSZ thermal barrier coatings exposed to gas flame, Surface and Coatings Technology 205 (2011) 4291.
[26] E.A.G. Shillington, D.R. Clarke, Spalling failure of a thermal barrier coating associated with aluminum depletion in the bond-coat, Acta Materialia 47 (1999) 1297.
[27] J.A. Haynes, M.K. Ferber, W.D. Porter, E.D. Rigney, Mechanical properties and fracture behavior of interfacial alumina scales on plasma-sprayed thermal barrier coatings, Materials at High Temperatures 16 (1999) 49.
[28] A.G. Evans, J.W. Hutchinson, On the mechanics of delamination and spalling in compressed films, International Journal of Solids and Structures 20 (1984) 455.
[29] H.H. Yu, M.Y. He, J.W. Hutchinson, Edge effects in thin film delamination, Acta Materialia 49 (2001) 93.